Title

Modeling nitrous oxide emission from rivers: a global assessment.

Authors

Hu, Minpeng
Chen, Dingjiang
Dahlgren, Randy A

Modeling nitrous oxide emission from rivers: a global assessment

MINPENG HU[1,2], DINGJIANG CHEN[1,3] and RANDY A. DAHLGREN[4]

[1]College of Environmental & Resource Sciences, Zhejiang University, Hangzhou 310058, China, [2]Zhejiang Provincial Key Laboratory of Subtropical Soil and Plant Nutrition, Zhejiang University, Hangzhou 310058, China, [3]Ministry of Education Key Laboratory of Environment Remediation and Ecological Health, Zhejiang University, Hangzhou 310058, China, [4]Department of Land, Air, and Water Resources, University of California, Davis, CA 95616, USA

Abstract

Estimates of global riverine nitrous oxide (N_2O) emissions contain great uncertainty. We conducted a meta-analysis incorporating 169 observations from published literature to estimate global riverine N_2O emission rates and emission factors. Riverine N_2O flux was significantly correlated with NH_4, NO_3 and DIN ($NH_4 + NO_3$) concentrations, loads and yields. The emission factors EF(a) (i.e., the ratio of N_2O emission rate and DIN load) and EF(b) (i.e., the ratio of N_2O and DIN concentrations) values were comparable and showed negative correlations with nitrogen concentration, load and yield and water discharge, but positive correlations with the dissolved organic carbon : DIN ratio. After individually evaluating 82 potential regression models based on EF(a) or EF(b) for global, temperate zone and subtropical zone datasets, a power function of DIN yield multiplied by watershed area was determined to provide the best fit between modeled and observed riverine N_2O emission rates (EF(a): $R^2 = 0.92$ for both global and climatic zone models, $n = 70$; EF(b): $R^2 = 0.91$ for global model and $R^2 = 0.90$ for climatic zone models, $n = 70$). Using recent estimates of DIN loads for 6400 rivers, models estimated global riverine N_2O emission rates of 29.6–35.3 (mean = 32.2) Gg N_2O–N yr^{-1} and emission factors of 0.16–0.19% (mean = 0.17%). Global riverine N_2O emission rates are forecasted to increase by 35%, 25%, 18% and 3% in 2050 compared to the 2000s under the Millennium Ecosystem Assessment's *Global Orchestration*, *Order from Strength*, *Technogarden*, and *Adapting Mosaic* scenarios, respectively. Previous studies may overestimate global riverine N_2O emission rates (300–2100 Gg N_2O–N yr^{-1}) because they ignore declining emission factor values with increasing nitrogen levels and channel size, as well as neglect differences in emission factors corresponding to different nitrogen forms. Riverine N_2O emission estimates will be further enhanced through refining emission factor estimates, extending measurements longitudinally along entire river networks and improving estimates of global riverine nitrogen loads.

Keywords: denitrification, global warming, greenhouse gases, nitrification, nitrous oxide, nitrous oxide emission factor

Received 27 October 2015; revised version received 10 April 2016 and accepted 1 May 2016

Introduction

Nitrous oxide (N_2O), which is responsible for ~9% of current global climate radiative forcing, has a global warming potential ~310 times that of carbon dioxide and a long residence time (~114 years) in the atmosphere (Hartmann *et al.*, 2013). Over the past half-century, human activities have approximately doubled the reactive nitrogen (N) addition on Earth resulting in saturation of the N assimilative capacity of some terrestrial ecosystems (Galloway *et al.*, 2004). This has led to a corresponding approximate doubling of riverine N loads (Green *et al.*, 2004). As a result, N_2O emission rates from rivers have increased, with an estimated 0.3–2.1 Tg N_2O–N yr^{-1} or 6–30% of global anthropogenic N_2O emissions (Seitzinger & Kroeze, 1998; Cole &

Caraco, 2001; Kroeze *et al.*, 2005; Beaulieu *et al.*, 2011; Syakila & Kroeze, 2011). Given projections for future increases in riverine N loads (Dumont *et al.*, 2005; Boyer *et al.*, 2006), modeling and predicting N_2O emissions from global rivers are critical for developing and refining the anthropogenic N_2O emission inventory and informing potential mitigation strategies.

Bottom-up emission inventories are typically used to estimate global and regional riverine N_2O emission rates, in which N_2O emission rates are calculated as the product of an emission factor and estimates of anthropogenic N loading to rivers (Ivens *et al.*, 2011; Outram & Hiscock, 2012). However, currently used emission factors for estimating global riverine N_2O emissions vary by one order of magnitude (i.e., 0.25–2.5%, Seitzinger & Kroeze, 1998; Seitzinger *et al.*, 2000; Cole & Caraco, 2001; Kroeze *et al.*, 2005; Beaulieu *et al.*, 2011; Syakila & Kroeze, 2011). Such a large variability for

Correspondence: Dingjiang Chen, tel/fax. +86 0571 88982071, e-mail: chendj@zju.edu.cn

emission factor values is mainly due to the local nature of riverine N_2O emission observations or from limited observations of $N_2O : N_2$ ratios for streams. For example, the two $N_2O : N_2$ ratios used in the estimates conducted by Seitzinger & Kroeze (1998) and Kroeze *et al.* (2005) were based on only four studies. Similarly, revision of the IPCC default emission factor in 2006 was based on measurements from two studies showing lower values (0.03–0.05%, Dong *et al.*, 2005; Clough *et al.*, 2006) for shorter streams in New Zealand and the United Kingdom and the supposition that longer rivers may have higher emission factors (De Klein *et al.*, 2006). Several studies argue that the current default IPCC emission factor (0.25%) may either overestimate (Clough *et al.*, 2007, 2011; Kroeze *et al.*, 2010) or underestimate (Beaulieu *et al.*, 2011; Yu *et al.*, 2013) and advocate the need to further evaluate emission factors for estimating global or regional riverine N_2O emission rates, although some observations support the current default IPCC emission factor value (Beaulieu *et al.*, 2008; Baulch *et al.*, 2011; Hinshaw & Dahlgren, 2013). Overall, the emission factor remains a major source of uncertainty in estimating regional or global N_2O emission rates (Nevison, 2000) and therefore requires further investigation, especially in a global context (Clough *et al.*, 2011; Turner *et al.*, 2015).

Riverine N_2O emissions result primarily from instream/hyporheic zone nitrification and denitrification (Seitzinger & Kroeze, 1998; Barnes & Owens, 1999), as well as possible direct N_2O input from sewage (Mosier *et al.*, 1998; Cébron *et al.*, 2005; Yu *et al.*, 2013) and groundwater (Mosier *et al.*, 1998; Clough *et al.*, 2006; Beaulieu *et al.*, 2008). Therefore, the N_2O flux, as well as the emission factor, is strongly dependent on a range of river attributes (e.g., temperature, water depth, wetted surface area, N concentration and forms, dissolved oxygen, pH, and microbially labile carbon, Outram & Hiscock, 2012; Venkiteswaran *et al.*, 2014; Clough *et al.*, 2007). For example, N_2O fluxes may be determined by ammonium concentration in some urban river networks (Yu *et al.*, 2013), while nitrate plays a more important role in agricultural watersheds (Beaulieu *et al.*, 2008; Baulch *et al.*, 2011; Hinshaw & Dahlgren, 2013). In addition, Rosamond *et al.* (2012) argued that widespread hypoxia is more conducive to higher N_2O emission flux from river systems than future increases in nitrate export to rivers. Several studies also indicate that N_2O flux decreases exponentially as a function of stream order (Garnier *et al.*, 2009; Turner *et al.*, 2015). As a result of temporal and spatial variability in stream hydro-biogeochemical characteristics, there are often large fluctuations in riverine N_2O fluxes, as well as emission factor, across time and space (Cole & Caraco, 2001; Reay *et al.*, 2003; Beaulieu *et al.*, 2008; Baulch

et al., 2011; Yang *et al.*, 2011; Harley *et al.*, 2015). Therefore, based on the limited and local nature of N_2O emissions, it is difficult to generalize the dominant factors regulating N_2O emissions at regional to global scales leading to large uncertainties in estimating riverine N_2O emissions at these larger scales (Outram & Hiscock, 2012; Rosamond *et al.*, 2012).

To address the limits and uncertainties implied in current global estimates of riverine N_2O emissions, this study conducted a meta-analysis that incorporates 169 observations of N_2O emissions and relevant variables from a range of rivers located on six continents and encompassing a range of climate zones and land-use types. In particular, this study (i) estimates three types of emission factors, (ii) addresses the factors controlling riverine N_2O fluxes and emission factors, (iii) develops models for predicting riverine N_2O emission rates, (iv) estimates global riverine N_2O emission rates and emission factor values, as well as their geographical distribution, and (v) forecasts global riverine N_2O rates for four future anthropogenic N load projections based on Millennium Ecosystem Assessment scenarios. As the first meta-analysis investigating riverine N_2O fluxes, this study improves our understanding of factors controlling riverine N_2O emissions at regional to global scales and provides a spatially explicit estimate for global riverine N_2O emissions.

Materials and methods

Data compilation

Data from 70 published studies between 1998 and 2016 that provided N_2O emissions from streams and rivers were compiled (Data S1, Table S1). For comparative purposes, we collected an additional 33, 104 and 43 records of N_2O fluxes in lakes/reservoirs, agricultural soils and wetlands, respectively, from another 68 published studies (Fig. S3). The following data criteria were applied: (i) Review papers and laboratory simulations were excluded; (ii) for multiple studies on the same river, we averaged the results of N_2O flux, emission factor and relevant variables for each year; (iii) for multiple observation sites and periods in a river, we averaged the results of N_2O fluxes, emission factor values, and relevant variables; (iv) for multiple measurement methods used in a river, we averaged the N_2O fluxes and emission factor values from the different methods; and (v) for different land-use divisions, the land use with a value >50% in the watershed was regarded as the dominant land-use type for the watershed (watersheds with highly mixed land use were <10%). The compiled database included 169 observations for N_2O fluxes, concentrations of nitrate (NO_3, 0.001–21.2 mg N L^{-1}), ammonium (NH_4, 0.001–12.5 mg N L^{-1}), dissolved inorganic N (DIN, 0.002–21.2 mg N L^{-1}), N_2O (0.01–15.5 µg N L^{-1}), dissolved oxygen (DO, 1.5–12.2 mg L^{-1}), and dissolved organic carbon (DOC, 0.26–31.5 mg L^{-1}), N_2O saturation (42–2500%),

river discharge (0.001–31710 m^3 s^{-1}) and water temperature (9.7–28.3 °C). The methods for measuring N$_2$O fluxes were floating chambers (14%), water–air gas exchange models (80%) and combined chambers and gas exchange models (9%). For observations using water–air exchange models, 8% were calculated by chemical tracers (Laursen & Seitzinger, 2002), 13% used a wind-exchange equation (Raymond & Cole, 2001), and 79% used a wind-stream turbulence equation (Clough *et al.*, 2007). The compiled database contains rivers on six continents and three representative climate zones (temperate, tropical and subtropical) (Fig. S1).

Calculation of N$_2$O emission factors

Due to the limited number of riverine N$_2$O emission factor values directly provided in the literature (<10), three methods were adopted to estimate emission factors in this study (Table 1). First, EF(a) was estimated by dividing the annual N$_2$O emission rate from a water body by the annual DIN load (Well *et al.*, 2005). The annual N$_2$O emission rate for a river was estimated as the product of the average N$_2$O flux and river water surface area. Second, EF(b) was estimated as the ratio of N$_2$O and DIN concentrations in the river water column, which can be used for estimating indirect N$_2$O emissions (De Klein *et al.*, 2006; Hinshaw & Dahlgren, 2013; Wang *et al.*, 2015). Third, EF(c) was estimated as the ratio of pN$_2$O (N$_2$O concentration in excess of equilibrium) and DIN concentration (Weiss & Price, 1980; Beaulieu *et al.*, 2008; Baulch *et al.*, 2012). Due to the unavailability of equilibrium N$_2$O concentration or pN$_2$O as well as specific data in the literature sources, we assumed constant atmospheric N$_2$O partial pressure (3.15 × 10^{-7} atm) and salinity (0‰) for all rivers in estimating equilibrium N$_2$O concentration (Weiss & Price, 1980) (Data S2). As the compiled observations contained data from rivers with mixed land-use types (implying N derived from multiple sources such as sewage discharge, leaching and runoff), the estimated EF(a), EF(b) and EF(c) values in this study may differ from the EF$_{5\text{-r}}$ proposed by the IPCC that separates the N

from leaching/runoff (i.e., nonpoint source pollution) and effluent from sewage and wastewater discharged into rivers (Doorn *et al.*, 2006).

Statistical and uncertainty analyses

All correlation, regression and nonparametric analyses were performed using SPSS (version 17.0, SPSS Inc., Chicago, IL, USA). N$_2$O flux and emission factors did not follow normal distributions according to the Kolmogorov–Smirnov test, $P < 0.001$ (Data S1, Fig. S2). Therefore, nonparametric tests were conducted for N$_2$O flux, emission factor, DO, discharge, N$_2$O saturation and NO$_3$/NH$_4$/DIN concentrations among different land-use types and climate zones. One-way ANOVA was conducted for water temperature, DOC : DIN ratio and N$_2$O concentration among different land-use types and climate zones after logarithmic or reciprocal transformation. Correlation and regression analyses were performed without transformation (Data S3).

To gain insight into the uncertainty of global riverine N$_2$O emission estimates, an uncertainty analysis was performed using Monte Carlo simulation (Data S5). Dissolved inorganic nitrogen loads for 6400 global rivers (McCrackin *et al.*, 2014) and parameters used in regression models for predicting N$_2$O emission rates were assumed to follow a normal distribution in the Monte Carlo simulations. A total of 10 000 Monte Carlo simulations were performed to obtain the mean and 95% confidence interval for N$_2$O emission rates in MATLAB (version 10.0; MathWorks Inc., Natick, MA, USA). To estimate the 95% confidence interval for global and regional emission factors, the 95% confidence intervals for N$_2$O emission rate and DIN leaching load were used for running 10 000 Monte Carlo simulations in Microsoft Excel 2007 embedded with Crystal Ball software (Professional Edition 2000; Oracle Ltd., Redwood City, CA, USA).

Results

Variability of riverine N$_2$O fluxes

Among the four types of ecosystems examined, N$_2$O fluxes followed (μg N$_2$O–N m^{-2} h^{-1}): wetlands (median: 44.0 ± 205.9, $n = 43$) > soils (median: 31.1 ± 42.6, $n = 104$) > rivers (median: 16.8 ± 679.4, $n = 169$) > lakes/reservoirs (median: 4.5 ± 14.3, $n = 33$) ($P < 0.05$, Data S1, Fig. S3). Compared to the other three ecosystems, riverine N$_2$O fluxes, ranging from −25 to 7440 μg N$_2$O–N m^{-2} h^{-1}, showed the largest spatial and temporal variability. Of the 169 riverine N$_2$O fluxes, 88% were positive and the remainder zero or negative implying that rivers are primarily a N$_2$O source. Riverine N$_2$O fluxes varied by dominant land-use type with higher fluxes (μg N$_2$O–N m^{-2} h^{-1}) observed in agricultural (25.1 ± 80.6, $n = 97$) and residential rivers (23.3 ± 9.6, $n = 31$) and lower values observed in forest rivers (6.7 ± 17.9, $n = 41$) ($P < 0.001$, Fig. 1a). Across the three

Table 1 Three methods for estimating N$_2$O emission factors

| Emission factors	Equation	Remarks
EF(a)	EF(a) = ER/L_{DIN}	ER is the annual N$_2$O emission rate (kg N$_2$O–N yr^{-1}), L_{DIN} is annual DIN load (kg N yr^{-1}), $n = 80$
EF(b)	EF(b) = c(N$_2$O)/ c(DIN)	c(N$_2$O) and c(DIN) denote dissolved N$_2$O (μg N$_2$O–N L^{-1}) and DIN concentrations (μg N L^{-1}), respectively; $n = 145$
EF(c)	EF(c) = c(pN$_2$O)/ c(DIN)	c(pN$_2$O) is dissolved N$_2$O concentration in excess of equilibrium with atmospheric N$_2$O concentrations (μg N$_2$O–N L^{-1}); $n = 113$
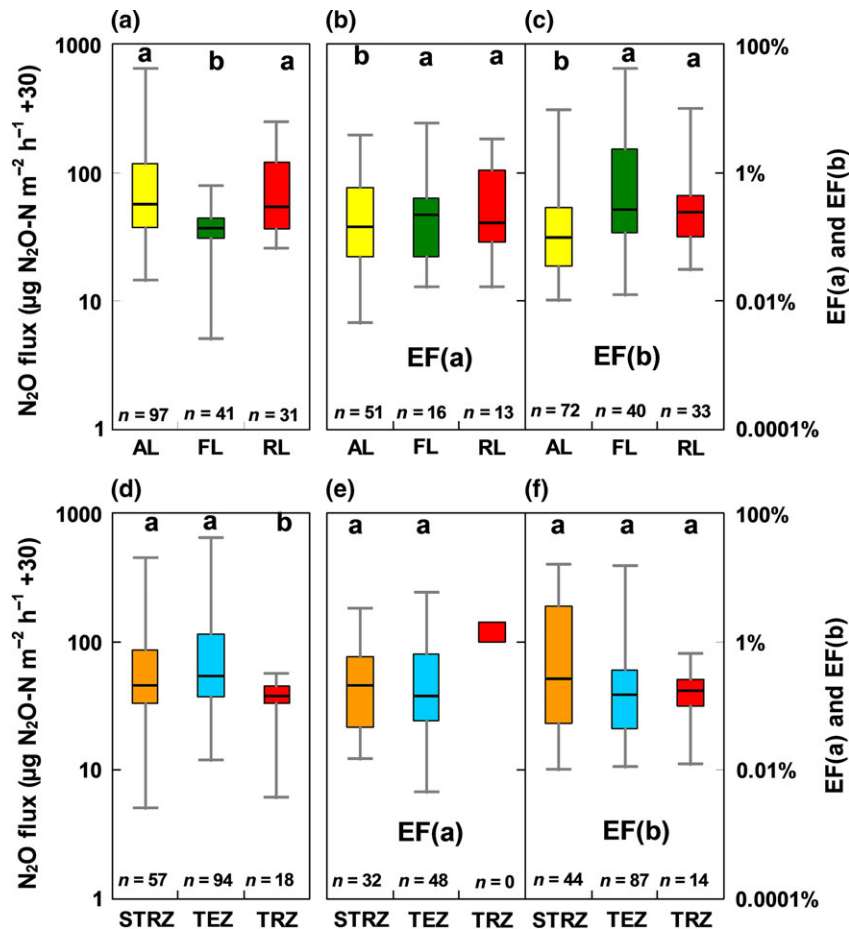
Fig. 1 Box plots of riverine N_2O (a) flux, (b) EF(a) and (c) EF(b) by watershed land use: AL (agricultural land), FL (forest land) and RL (residential land) and riverine N_2O (d) flux, (e) EF(a) and (f) EF(b) by climate zones: STR (subtropical), TR (tropical) and TE (temperate). Lower case letters above bars denote significant differences.

climate zones, higher N_2O emission fluxes (μg N_2O–N m^{-2} h^{-1}) occurred in temperate (25.9 ± 489.5, $n = 94$) and subtropical rivers (16.3 ± 983.4, $n = 57$) than in tropical rivers (7.3 ± 12.7, $n = 18$) ($P < 0.01$, Fig. 1c). Consistent with the higher N_2O fluxes, agricultural and residential rivers, as well as temperate and subtropical rivers, had higher concentrations of dissolved N_2O, NH_4, NO_3 and DIN than forest and tropical rivers ($P < 0.001$) (Figs 2 and 3).

Riverine N_2O fluxes showed significant positive correlations ($P < 0.05$) with dissolved N_2O concentration, N_2O saturation, and NH_4, NO_3 and DIN concentrations, loads and yields, while it was negatively correlated with DOC : DIN ratio and DO concentration (Data S3, Table S2). However, no significant correlations were observed between N_2O flux and water temperature ($P = 0.26$, $n = 118$), water discharge ($P = 0.38$, $n = 145$) or watershed area ($P = 0.68$, $n = 105$, Table S2). The NO_3, NH_4 and DIN concentrations explained 36%, 14% and 37% of the global variability in

N_2O fluxes, respectively (Table S2). The combined NO_3 and NH_4 concentrations explained 35% of the variability in N_2O fluxes (Table S2). Except for forest rivers ($P > 0.05$), NH_4 concentration was significantly correlated with N_2O fluxes in residential and agricultural rivers (Table S3). Although N_2O flux and DIN or NO_3 concentrations were significantly correlated in both agricultural and residential rivers, only a weak significant correlation was found in forest rivers (Table S3). Although NO_3, NH_4 and DIN concentrations presented significant correlations with N_2O emission fluxes in individual climate zones, temperate rivers showed stronger correlations between N concentrations and N_2O flux than subtropical/tropical rivers (Table S4).

Variability of riverine N_2O emission factors

Estimated EF(a) values ranged from 0.005% to 7.13% (median: $0.15 \pm 1.23\%$, $n = 80$, Data S2, Fig. S4a) and were similar to median EF(b) values (range: 0.003–41%,
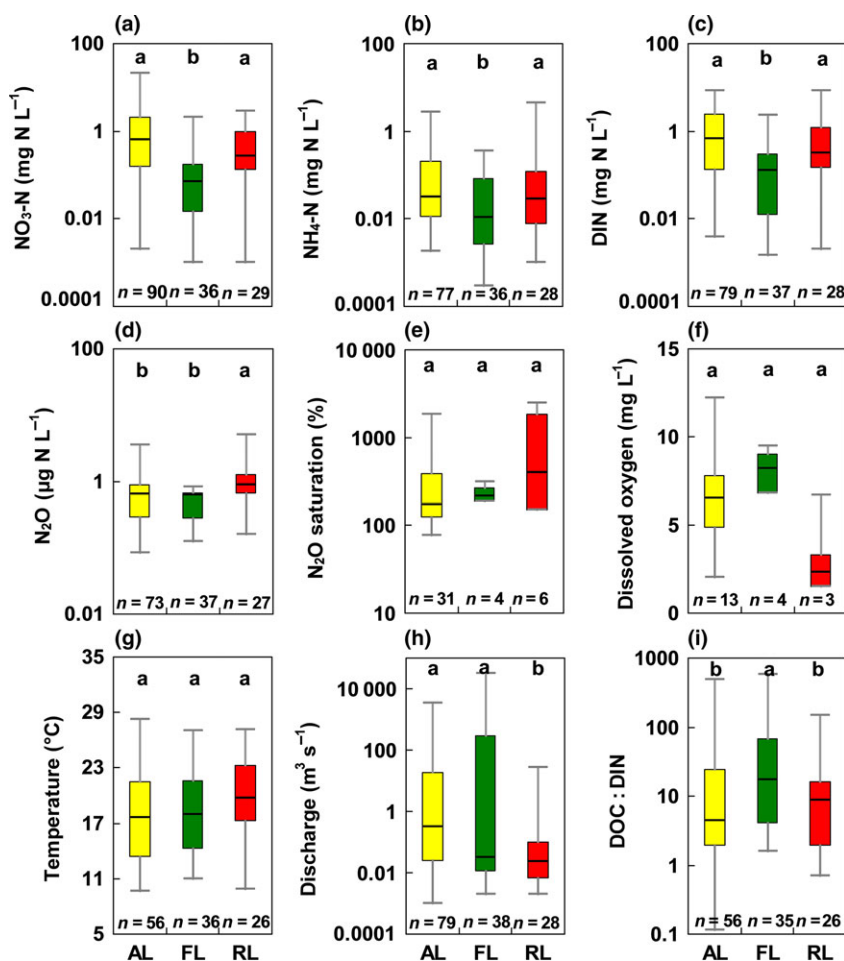
Fig. 2 Box plots of riverine (a) nitrate, (b) ammonium, (c) dissolved inorganic nitrogen (DIN), (d) N$_2$O concentration, (e) N$_2$O saturation, (f) dissolved oxygen, (g) water temperature, (h) water discharge and (i) ratio of dissolved organic carbon (DOC) and DIN by watershed land use: AL (agricultural lands), FL (forest lands) and RL (residential lands). Lower case letters above bars denote significant differences.

median: $0.17 \pm 6.0\%$, $n = 145$). The estimated N$_2$O flux using EF(b) was comparable with the average N$_2$O flux reported in the literature (Fig. S4b). Estimated EF(c) values ranged from -0.91% to 3.63% (median: $0.04 \pm 0.50\%$, $n = 113$, Fig. S4a). The estimated N$_2$O flux using EF(c) was one order of magnitude lower than the average N$_2$O flux reported in the literature (Fig. S4b). Sensitivity analysis (Fig. S5) indicated that the lower estimate likely results from the lack of direct data for atmospheric N$_2$O partial pressure and salinity (both set to constant values for all rivers) in estimating equilibrium N$_2$O concentrations. These results indicate that the EF(c) method may not be applicable in our analysis due to the lack of available data from literature sources to make accurate calculations. Therefore, we used EF(a) and EF(b) in the following analyses.

The EF(a) and EF(b) values for the three land-use divisions followed (Fig. 1a): forest rivers ($0.28 \pm$

1.42% for EF(a), $n = 16$; $0.27 \pm 9.1\%$ for EF(b), $n = 40$) > residential rivers ($0.16 \pm 1.08\%$ for EF(a), $n = 13$; $0.19 \pm 6.0\%$ for EF(b), $n = 33$) > agricultural rivers ($0.14 \pm 1.23\%$ for EF(a), $n = 51$; $0.08 \pm 2.8\%$ for EF(b), $n = 72$). The EF(a) and EF(b) values showed no significant differences among the three climate zones (Fig. 1d). The distribution of EF(a) and EF(b) values across residential, agricultural and forest rivers followed a similar pattern to the distribution of DOC : DIN, but an inverse pattern with the distribution of NH$_4$, NO$_3$ and DIN concentrations and river discharge (Fig. 2h, i). Further statistical analyses showed that EF(a) and EF(b) had negative correlations with river discharge and watershed area, but a positive correlation with DOC:DIN (Table S2). Furthermore, EF(a) and EF(b) rapidly decreased with increasing NH$_4$, NO$_3$ and DIN concentrations, loads and yields and DOC concentration (Table S2). The correlation between EF(a)
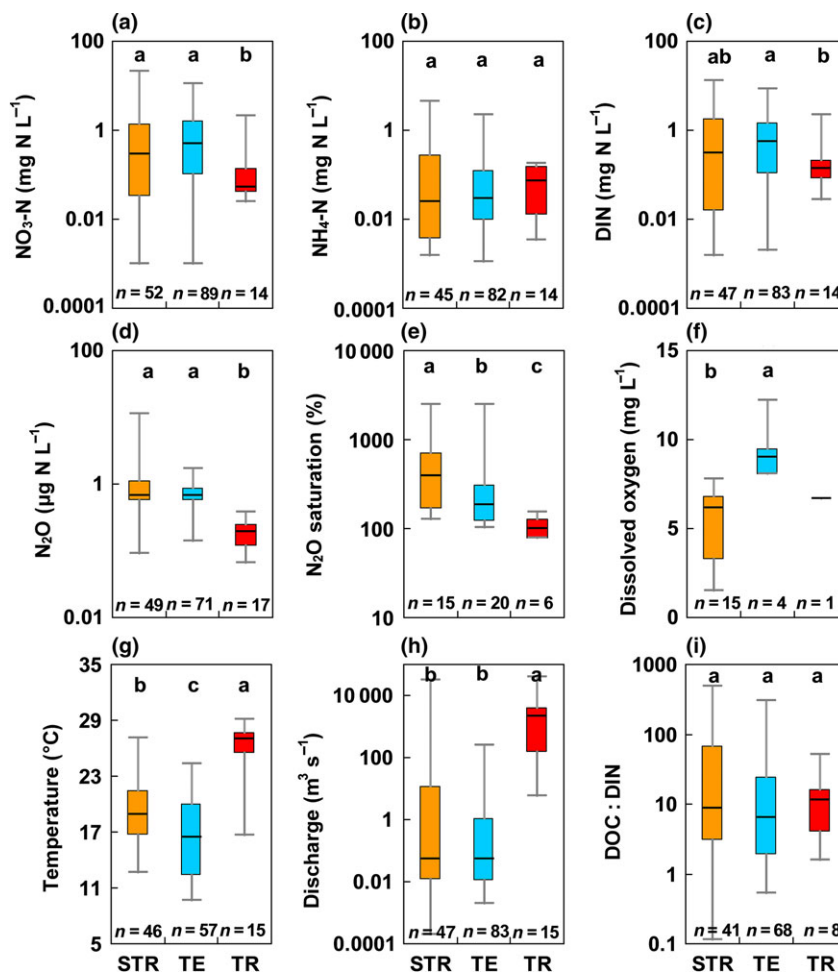
Fig. 3 Box plots of riverine (a) nitrate, (b) ammonium, (c) dissolved inorganic nitrogen (DIN), (d) N_2O concentration, (e) N_2O saturation, (f) dissolved oxygen, (g) water temperature, (h) water discharge and (i) ratio of dissolved organic carbon (DOC) and DIN by climate zone: STR (subtropical), TR (tropical) and TE (temperate). Lower case letters above bars denote significant differences.

or EF(b) and discharge in forest rivers was higher than for agricultural and residential rivers (Table S3), while temperate rivers had lower correlations than subtropical/tropical rivers (Table S4). No significant correlations were observed between EF(a) or EF(b) and dissolved N_2O concentration, N_2O saturation, water temperature and DO (Table S2).

Regression models for riverine N_2O emission rates

Riverine N_2O emission rates (kg N_2O–N yr^{-1}) can be estimated as the product of the emission factor and riverine DIN load (Well *et al.*, 2005; De Klein *et al.*, 2006). Our analyses indicate that variability of EF(a) or EF(b) is related to a range of factors, such as N concentrations, loads and yields, DOC : DIN, DOC concentration, discharge and watershed area (Table S2). Exploratory multiple regression analyses were

conducted for predicting EF(a) or EF(b) using various combinations of these factors and different functions. The resulting 82 models explained <0.01–99% of the variability in EF(a) as well as N_2O emission rates with a large percent bias coefficient range (<−100 to >100, Data S3, Fig. 4a; Table S5). Combining N concentration, load or yield with DOC concentration, DOC : DIN and/or discharge did not significantly improve the model accuracy compared to the model incorporating only N concentration, load or yield. The lack of improvement mainly results from significant correlations ($P < 0.05$) between NH_4, NO_3, DIN concentration, load or yield and DOC concentration ($R^2 = 0.10$–0.49, $n = 53$–56), DOC : DIN ($R^2 = 0.22$–0.78, $n = 53$–56) and discharge ($R^2 = 0.30$–0.90, $n = 65$–76). Among them, DIN yield (Y_{DIN}, kg N yr^{-1} km^{-2}) best explained variability of EF (a) as well as N_2O emission rate (Eqn 1, $R^2 = 0.92$, $P < 0.001$, $n = 70$; Fig. 4a and Table S5):
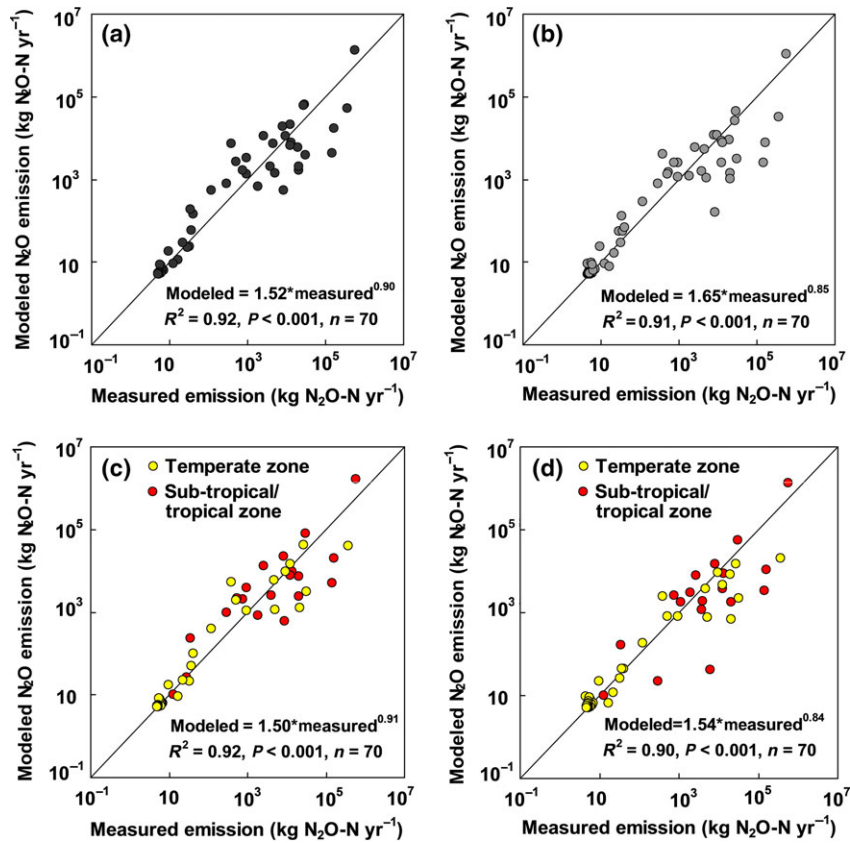
Fig. 4 (a) Modeled (Eqn 1) vs. measured riverine N$_2$O emission rates, (b) modeled (Eqn 2) vs. measured riverine N$_2$O emission rates, (c) modeled (Eqns 3 and 4) vs. measured riverine N$_2$O emission rates, (d) modeled (Eqns 5 and 6) vs. measured riverine N$_2$O emission rates

$$\text{ER} = 0.0034 Y_{\text{DIN}}^{-0.169} L_{\text{DIN}} = 0.0034 Y_{\text{DIN}}^{0.831} A \qquad (1)$$

where ER is riverine N$_2$O emission rate (kg N$_2$O–N yr^{-1}), L_{DIN} is DIN load (kg N yr^{-1}), and A is watershed area (km^2).

The resulting 82 models explained <1–99% of the variability in EF(b) (Data S3, Table S8) and <0.01–91% of the variability in N$_2$O emission rates based on EF(b) values with a large percent bias coefficient range (<−100 to >100, Table S8). Similar to EF(a), the model using DIN yield (Y_{DIN}, kg N yr^{-1} km^{-2}) as an independent variable for explaining variability of EF(b) presented the highest agreement between modeled and measured N$_2$O emission rates ($R^2 = 0.91$, percent bias coefficient = 14.0, $P < 0.001$, $n = 70$; Fig. 4b and Table S8):

$$\text{ER} = 0.0138 Y_{\text{DIN}}^{-0.417} L_{\text{DIN}} = 0.0138 Y_{\text{DIN}}^{0.583} A \qquad (2)$$

Considering the response of EF(a) and EF(b) to changes in potential influencing factors among the three climate zones (Table S4), the 82 potential regression models were further evaluated for their ability to determine N$_2$O rates for subtropical/tropical and

temperate river systems. Similar to the global analysis, the model using DIN yield as an independent variable best explained variability of EF(a) as well as N$_2$O emission rates for subtropical/tropical rivers (Eqn 3, $R^2 = 0.85$, percent bias coefficient = −78.5, $P < 0.001$, $n = 30$; Fig. 4c and Table S6) and for temperate rivers (Eqn 4, $R^2 = 0.88$, percent bias coefficient = 72.4, $P < 0.001$, $n = 40$; Fig. 4c and Table S7):

$$\text{ER}_{\text{st}} = 0.0044 Y_{\text{DIN}}^{-0.179} L_{\text{DIN}} = 0.0044 Y_{\text{DIN}}^{0.821} A \qquad (3)$$

$$\text{ER}_{\text{t}} = 0.0041 Y_{\text{DIN}}^{-0.230} L_{\text{DIN}} = 0.0041 Y_{\text{DIN}}^{0.770} A \qquad (4)$$

where ER$_{\text{st}}$ and ER$_{\text{t}}$ are riverine N$_2$O emission rates (kg N$_2$O–N yr^{-1}) in subtropical/tropical and temperate zones, respectively. Furthermore, the model using DIN yield as an independent variable for explaining variability of EF(b) demonstrated the highest agreement between modeled and measured N$_2$O emission rates for subtropical/tropical rivers (Eqn 5, $R^2 = 0.73$, percent bias coefficient = −45.3, $P < 0.001$, $n = 30$; Fig. 4d and Table S9) and for temperate rivers (Eqn 6, $R^2 = 0.94$, percent bias coefficient = 90.0, $P < 0.001$, $n = 40$; Fig. 4d and Table S10):

$$ER_{st} = 0.0112Y_{DIN}^{-0.355}L_{DIN} = 0.0112Y_{DIN}^{0.645}A \qquad (5)$$

$$ER_t = 0.0198Y_{DIN}^{-0.521}L_{DIN} = 0.0198Y_{DIN}^{0.479}A \qquad (6)$$

Estimation of global riverine N$_2$O emission

Using model Eqns (1)–(6) and DIN loads for 6400 global rivers recently calculated by the NEWS2-DIN-S model (McCrackin *et al.*, 2014), we estimated global riverine N$_2$O emissions. The estimated 18.84 Tg N yr^{-1} of global riverine DIN load yielded a global riverine N$_2$O emission rate of 32.2 (95% CI: 12.4–66.9) Gg N$_2$O–N yr^{-1}, which is the average of four modeling approaches (Table 2): 29.4 (95% CI: 12.0–58.1) Gg N$_2$O–N yr^{-1} using Eqn (1), 30.4 (95% CI: 14.2–53.9) Gg N$_2$O–N yr^{-1} using Eqn (2), 35.3 (95% CI: 10.8–85.0) Gg N$_2$O–N yr^{-1} using Eqns (3) and (4) and 33.8 (95% CI: 12.8–70.7) Gg N$_2$O–N yr^{-1} using Eqns (5) and (6). Rivers in Asia presented the largest N$_2$O emission rate (10.6 Gg N$_2$O–N yr^{-1}) and accounted for 33% of global emissions relative to 29% of global land area. The lowest N$_2$O emission rate was in Oceania (including Australia) with a mean of 1.3 Gg N$_2$O–N yr^{-1} representing 4% of global emissions relative to 6% of global land area. Estimated mean N$_2$O emission rates from rivers in Europe, Africa, North America and South America accounted for 15–20% of global N$_2$O emissions. Global N$_2$O emission yields displayed considerable spatial variation over the 6400 basins with an average of 0.24 kg N$_2$O–N km^{-2} yr^{-1} (Fig. 5a). Generally, higher riverine N$_2$O emission yields were observed in agriculturally intensive regions (such as the Mississippi River Basin and South-East Asia), densely populated areas (such as Western Europe and South Asia) and some tropical rainforest regions (such as the Amazon and Congo River basins). The higher DIN loads in subtropical/tropical rivers yielded much more N$_2$O (79%) than temperate/frigid rivers (21%).

The estimated global mean emission factor (i.e., the ratio between estimated global riverine N$_2$O emission rate and DIN load) from the average of the four modeling approaches was 0.17% (95% CI: 0.08–0.31%; Table 2): 0.16% (95% CI: 0.08–0.27%) from Eqn (1), 0.16% (95% CI: 0.08–0.30%) from Eqn (2), 0.19% (95% CI: 0.08–0.34%) from Eqns (3) and (4) and 0.18% (95% CI: 0.08%–0.32%) from Eqns (5) and (6). The estimated mean emission factor of 0.19% (95% CI: 0.08–0.36%) in subtropical/tropical rivers was comparable to the 0.17% (95% CI: 0.08–0.32%) observed in temperate/frigid rivers. Australia had the highest emission factor value of 0.25% (95% CI: 0.13–0.41%), while the estimated values for Asia, Africa, Europe, South America and North America were relatively similar (0.16–0.19%, Table 2). Across the 6400 global rivers, estimated emission factor values varied by more than two orders of magnitude, with higher emission factors in river networks with lower DIN yield and water discharge (Fig. 5b).

Prediction of future global riverine N$_2$O emissions

Global riverine N$_2$O emission rates in 2050 were forecasted based on future riverine N load projections from the Millennium Ecosystem Assessment [*Global*

Table 2 Modeled global riverine N$_2$O emission rates and emission factors across continents and climate zones

Continent or climate zone	Runoff (mm yr^{-1})	DIN leaching (Tg N yr^{-1})	N$_2$O emission (Gg N$_2$O–N yr^{-1})	Emission factor (%)
Asia	246	6.68 [6.09, 7.34]	10.61 [4.62, 19.99]	0.16 [0.08, 0.26]
Europe	233	2.16 [1.97, 2.37]	3.41 [1.48, 6.39]	0.16 [0.08, 0.26]
Africa	195	2.97 [2.71, 3.25]	5.55 [2.47, 10.23]	0.18 [0.08, 0.30]
South America	561	3.73 [3.40, 4.09]	6.30 [2.75, 11.84]	0.17 [0.08, 0.28]
North America	264	2.53 [2.30, 2.78]	4.93 [2.20, 9.13]	0.19 [0.09, 0.31]
Oceania	288	0.79 [0.49, 1.25]	1.34 [0.59, 2.52]	0.23 [0.13, 0.41]
Australia	67	0.21 [0.13, 0.33]	0.53 [0.25, 0.96]	0.25 [0.13, 0.41]
Subtropical/tropical	322	14.96 [9.42, 23.78]	25.35 [8.45, 57.87]	0.19 [0.08, 0.36]
Temperate/frigid	190	3.89 [2.45, 6.18]	6.87 [2.58, 14.65]	0.17 [0.08, 0.32]
Global*	282	18.87 [12.63, 29.21]	29.41 [12.01, 58.09]	0.16 [0.08, 0.27]
Global†			30.35 [14.17, 53.85]	0.16 [0.08, 0.30]
Global‡			35.27 [10.78, 84.95]	0.18 [0.08, 0.32]
Global§			33.76 [12.79, 70.65]	0.19 [0.08, 0.34]

Number in each bracket denotes the 95% confidence interval from Monte Carlo simulation.
*Estimated by Eqn (1).
†Estimated by Eqn (2).
‡Estimated by Eqns (3) and (4).
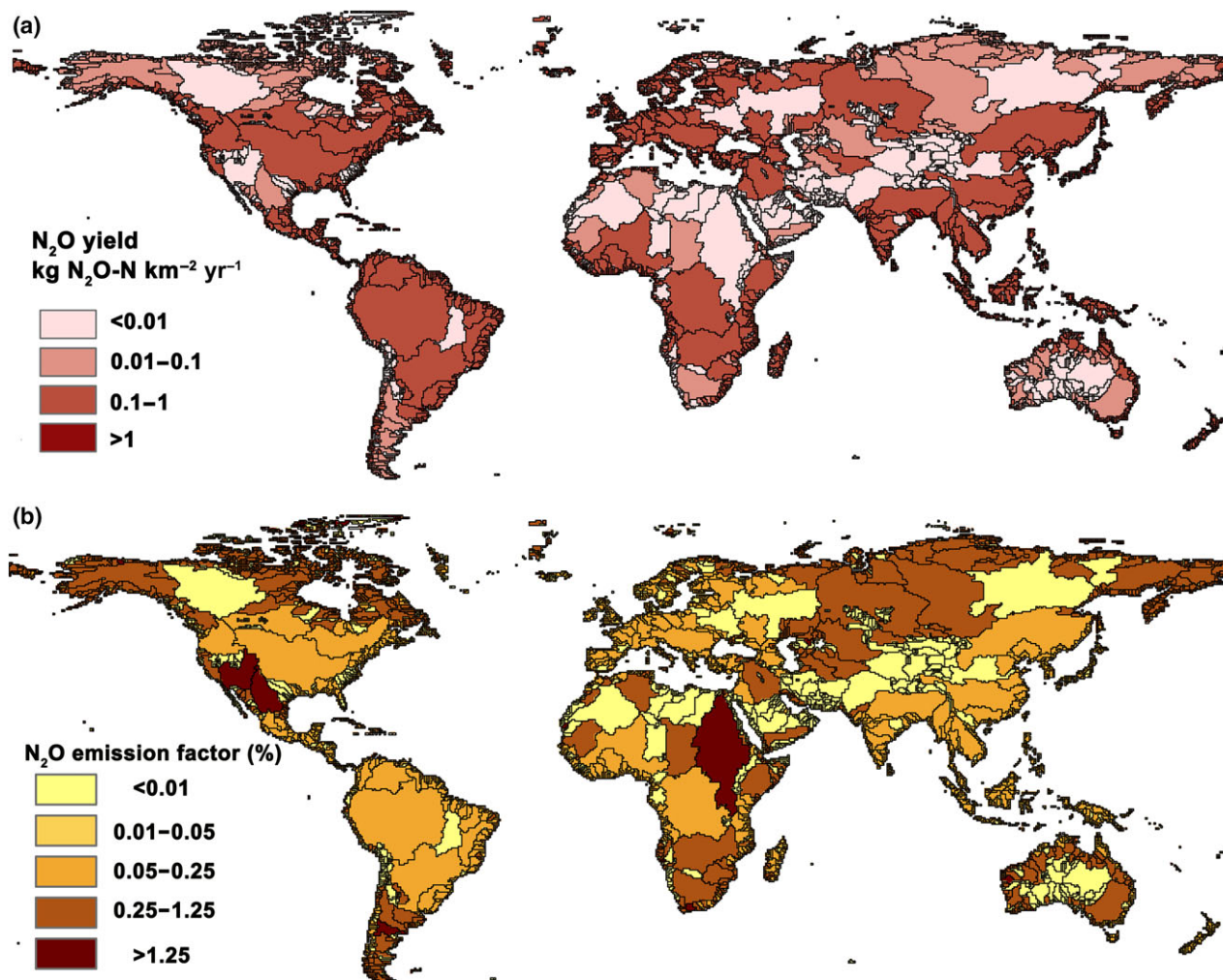§Estimated by Eqns (5) and (6); other values are average from the four modeling approaches.

(a)

N₂O yield
kg N₂O-N km⁻² yr⁻¹

- <0.01
- 0.01–0.1
- 0.1–1
- >1

(b)

N₂O emission factor (%)

- <0.01
- 0.01–0.05
- 0.05–0.25
- 0.25–1.25
- >1.25

Fig. 5 Global distributions of riverine N₂O (a) emission yield and (b) emission factor for 2000s.

Orchestration (GO), *Order from Strength* (OS), *Technogarden* (TG) and *Adapting Mosaic* (AM)] (Data S6, Alcamo *et al.*, 2005). These four scenarios differ in future development strategies (globalization or regionalization) and attitudes toward environmental issues and ecosystem management (proactive or reactive): (i) globalization: GO and TG; (ii) regionalization: OS and AM; (iii) reactive ecosystem management: GO and OS; and (iv) proactive ecosystem management: TG and AM (Alcamo *et al.*, 2005). A previous study predicted that global riverine DIN loads would increase 47% for GO, 28% for OS and 10% for TG, while decreasing by 8% for AM in 2050 compared to the 2000s (Kroeze *et al.*, 2010).

Using the predicted changes for global riverine DIN loads, the average of the four modeling approaches predicted that average global riverine N₂O emission rates would be 43.4, 40.2, 38.0 and 33.1 Gg N₂O–N yr⁻¹ in

2050 for the GO, OS, TG and AM scenarios, respectively (Fig. 6). These predictions represent an increase of 35%, 25%, 18% and 3% compared to the 2000s baseline, respectively. The continental trends differ considerably from global trends. Riverine N₂O emission rates in Oceania, South America and Africa would continue to increase in 2050 under the four scenarios, with Africa having the highest percentage increase (Fig. 6a). N₂O emissions in Asia and Europe would decrease in 2050 under both TG and AM scenarios. Each continent presents an increasing trend in 2050 under both GO and OS scenarios with Europe having the lowest percentage increase. Among the climate zones, subtropical/tropical rivers represent a 5–42% increase for the four scenarios, while temperate/frigid rivers would increase 18% and 11% and decrease 3% and 8% in 2050 for the GO, OS, TG and AM scenarios, respectively (Fig. 6b).
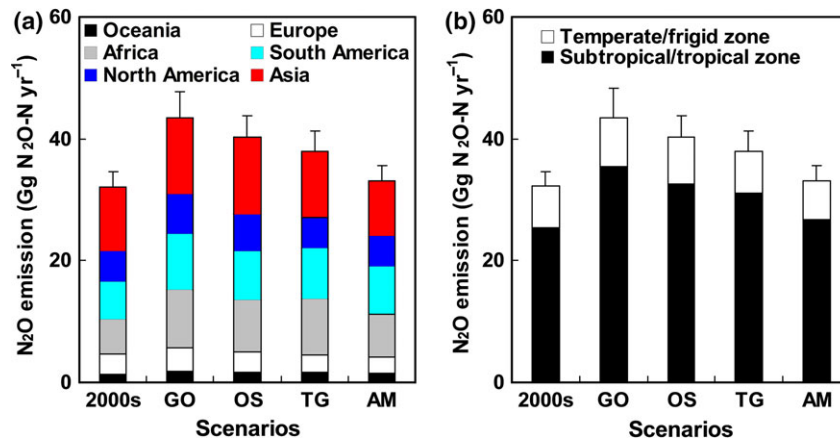
Fig. 6 Predicted average global riverine N₂O emission rates across (a) continents and (b) climate zones in 2050 using the Global Orchestration (GO), Order from Strength (OS), Technogarden (TG) and Adapting Mosaic (AM) scenarios from the Millennium Ecosystem Assessment. The error bar denotes standard error of the average values from the four modeling approaches.

Discussion

Controls on the riverine N₂O flux

Although riverine N₂O flux displays a high variability (Fig. 1a), it showed a strong correlation with NH_4, NO_3 and DIN concentration, load and yield (Table S2), suggesting that the magnitude of N₂O emission fluxes is mainly determined by the available N level in river systems, consistent with results reported in several previous studies (McMahon & Dennehy, 1999; Stow *et al.*, 2005; Clough *et al.*, 2011; Yu *et al.*, 2013). The high dependence of N₂O flux on both NH_4 and NO_3 levels further implies that N₂O emission from rivers is derived from both nitrification and denitrification processes (Seitzinger *et al.*, 2000; Cole & Caraco, 2001; Rosamond *et al.*, 2012; Hinshaw & Dahlgren, 2013). Due to the role of both nitrification and denitrification, N₂O emission fluxes demonstrated a higher correlation with DIN concentrations than with either NH_4 or NO_3 concentrations alone (Table S2). In contrast, forest rivers had weak correlations between N₂O flux and concentrations of different N forms (Table S3) implying that other factors, such as DO, microbial carbon sources or pH, had a stronger control on N₂O production from coupled nitrification–denitrification (Sobczak *et al.*, 2003; Van Den Heuvel *et al.*, 2011; Rosamond *et al.*, 2012; Yu *et al.*, 2013; Venkiteswaran *et al.*, 2014). Nitrification and denitrification reaction kinetics are controlled by the availability of terminal electron donors (NH_4 and labile DOC) and acceptors (O_2 and NO_3) (Hedin *et al.*, 1998; Zarnetske *et al.*, 2012). The forest rivers had significantly lower NH_4 and NO_3 concentrations and higher DOC and dissolved O_2 concentrations than the other systems (Fig. 2) potentially resulting in

NH_4 and NO_3 being dominated by DOC and O_2 as electron donor and acceptor, respectively. Higher DO concentration in forest rivers may also attenuate denitrification rates because denitrifying microbes are usually facultative anaerobes (Christensen *et al.*, 1990; Cébron *et al.*, 2005; Rosamond *et al.*, 2012). Given that forest ecosystems often occur in lower ordered river systems (i.e., headwater catchments, Fig. 2), channel geomorphology will likely be highly variable among forest rivers leading to greater variability in hyporheic characteristics contributing to nitrification and denitrification.

Several studies have shown that nitrification rates can be greater than denitrification rates in rivers (Holmes *et al.*, 1996; Webster *et al.*, 2003; Arango & Tank, 2008). The IPCC assumption states that nitrification produces twice as much N₂O per unit N converted as compared to denitrification (Mosier *et al.*, 1998). However, the relative contribution of riverine nitrification and denitrification to N₂O production varies with land use due to varying substrate delivery, river characteristics and resulting *in situ* processes (Hemond & Duran, 1989; Cébron *et al.*, 2005; Toyoda *et al.*, 2009; Beaulieu *et al.*, 2010). A weaker correlation was found between NO_3 concentration and N₂O flux than between NH_4 concentration and N₂O flux in residential rivers (Table S3) implying that nitrification and nitrifier denitrification might produce a greater N₂O flux than denitrification in residential rivers (Beaulieu *et al.*, 2010; Yu *et al.*, 2013). N₂O production by nitrification at the water–bed interface can be enhanced with decreasing DO concentrations due to incomplete aerobic nitrification (Cébron *et al.*, 2005). In parallel, nitrifier denitrification, a pathway of nitrification in which NH_4^+ is oxidized to NO_2^- followed by the reduction in NO_2^- to

N$_2$O and N$_2$, can also account for N$_2$O production under high NH$_4$ loadings in association with low DO (Toyoda *et al.*, 2009). In the lower Seine River and estuary, for example, nitrification and nitrifier denitrification were found to be the dominant N$_2$O-forming processes, and they were kinetically favorable under optimal DO concentrations of 1.1–1.5 mg O$_2$ L^{-1} (Cébron *et al.*, 2005), which is comparable with DO concentrations observed in many residential rivers in this study (Fig. 2f). In contrast, the stronger correlation between NO$_3$ concentration and N$_2$O flux compared to NH$_4$ concentration vs. N$_2$O flux in agricultural rivers (Table S3) implies that denitrification might produce a greater N$_2$O contribution than nitrification (Clough *et al.*, 2007; Yan *et al.*, 2012). As 57% of our observations are from agricultural rivers (Table S1), the negative correlation observed between DO and N$_2$O flux in this study (Table S2) implies a role for hypoxia or denitrification in N$_2$O production (Rosamond *et al.*, 2012). Denitrification tends to occur in the top few centimeters of anoxic sediments where NO$_3$ is supplied by NO$_3$ diffusion from the water column and nitrification processes in the oxic surface layer of sediments (Barnes & Owens, 1999). Thus, a high NO$_3$ concentration in agricultural rivers (Fig. 2a) potentially stimulates denitrification and N$_2$O production (Clough *et al.*, 2007; Yan *et al.*, 2012). The higher correlation between NO$_3$ concentration and N$_2$O flux than that between NH$_4$ concentration and N$_2$O flux in both temperate/frigid and subtropical/tropical rivers (Table S4) suggests that climate is not a strong factor influencing N$_2$O contributions from nitrification vs. denitrification among climate zones. A global meta-analysis also indicated that elevated temperature had no significant effect on soil N$_2$O emission flux (Barnard *et al.*, 2005).

Controls on the riverine N$_2$O emission factors

The significant negative correlation between EF(a) or EF(b) and water discharge as well as watershed area (Table S2) suggests that N$_2$O production or evasion efficiency is decreased with increasing river channel size. This result is consistent with the current understanding of hydrologic/geomorphic controls on in-stream/hyporheic nitrification and denitrification processes (Alexander *et al.*, 2000; Peterson *et al.*, 2001; Mulholland *et al.*, 2008). Increasing river water discharge decreases the water–bed contact area per unit water volume and decreases the efficiency of nitrate diffusion across the river water–sediment interface leading to lower denitrification and/or nitrification per unit N loading (Alexander *et al.*, 2000; Peterson *et al.*, 2001; Mulholland *et al.*, 2008). In addition, increasing river discharge decreases the water residence time, decreasing the

opportunity and duration for nitrification and denitrification (Chen *et al.*, 2011; McCrackin *et al.*, 2014). The gas transfer velocity rate that determines the evasion efficiency across the water–atmosphere interface with supersaturated N$_2$O decreases with increasing river order due to declining water turbulence with increasing river order (increasing water volume buffering capacity) (Garnier *et al.*, 2009; Raymond *et al.*, 2012; Turner *et al.*, 2015). All these mechanisms suggest that the proximity of N sources to small rivers might be a major factor regulating N$_2$O production along a river network.

The negative relationship between EF(a) or EF(b) and N concentrations, loads and yields (Table S2) is consistent with several previous studies (Beaulieu *et al.*, 2011; Hinshaw & Dahlgren, 2013). This negative relationship primarily results from decreasing denitrification and nitrification efficiency with increasing N inputs due to progressive biological saturation (Bernot & Dodds, 2005; O'Brien *et al.*, 2007; Mulholland *et al.*, 2008, 2009). This is consistent with batch and continuous flow experiments in the lower Seine River that indicated N$_2$O production by the nitrifier-denitrification process was fit by a Michaelis–Menten saturation function (Cébron *et al.*, 2005). It is suggested that the number of favorable denitrification and nitrification sites at the river water–bed interface is relatively constant, resulting in progressive biological saturation for processing N with increasing N loading (Peterson *et al.*, 2001; Bernot *et al.*, 2006; Mulholland *et al.*, 2008; Aguilera *et al.*, 2013). Although there was a negative correlation between EF(a) or EF(b) and DOC concentration, a positive correlation was observed between EF(a) or EF(b) and the DOC : DIN ratio (Table S2) suggesting that available C relative to N plays an important role in regulating N$_2$O production efficiency. Previous studies suggest that nitrification is dominant at low C : N ratios, while nitrification is inhibited at high C : N ratios as available C increases microbial activity and O$_2$ consumption leading to low DO conditions favorable for denitrification (Payne, 1981; Beauchamp *et al.*, 1989; Her & Huang, 1995; Miller *et al.*, 2008). Forest rivers had higher EF(a) and EF(b) values than residential and agricultural rivers, possibly because of the higher DOC : DIN ratio or smaller channel size (Fig. 2). However, the higher EF(a) and EF(b) observed in forest rivers might also be associated with near atmospheric N$_2$O equilibrium concentration and low DIN concentration (Beaulieu *et al.*, 2008; Baulch *et al.*, 2012). Given the higher EF(a) and EF(b) values, forest headwater streams may act as important locations for producing N$_2$O, particularly in developing regions where atmospheric DIN deposition has increased rapidly in recent decades and will continue to increase in the future

(Matson *et al.*, 2002; Liu *et al.*, 2013). Although in-stream nitrification and denitrification efficiency is usually influenced by temperature (Clough *et al.*, 2007; Xia *et al.*, 2013; McCrackin *et al.*, 2014; Venkiteswaran *et al.*, 2014), this study suggests that temperature is not a dominant driver of global N_2O emission factor variability as indicated by the lack of significant differences for EF(a) or EF(b) among climate zones (Fig. 1d) and between EF(a) or EF(b) and temperature (Table S2).

Comparison with previous estimates of global riverine N_2O emissions

The models developed in this study (Eqns 1–6 – power functions of DIN yield multiplied by watershed area) showed reasonably high accuracy and robustness for predicting riverine N_2O emission rates across the wide range of metadata (Fig. 4). Similar power function relationships between riverine N_2O flux and N concentrations have been applied to field observations (McMahon & Dennehy, 1999; Stow *et al.*, 2005; Beaulieu *et al.*, 2011; Clough *et al.*, 2011; Yu *et al.*, 2013). Models developed using EF(a) and EF(b) for global and individual climate zone datasets produced comparable estimates for global N_2O emission rates and emission factors (Table 2), which further verifies their global suitability and robustness. These models only require data for riverine DIN yield and watershed area, thus providing a simple, efficient and robust tool for estimating global or regional riverine N_2O emission rates.

This study provides the first spatially explicit estimate of emission factors for global rivers (Table 2 and Fig. 5b), which further offers a geographical distribution of N_2O emission potentials across global rivers. Model results indicate that Asian rivers have the highest contribution to total N_2O emissions (Table 2), which is consistent with previous global estimates (Kroeze *et al.*, 2005, 2010). Spatially, high N_2O emission yields (>0.1 kg N_2O–N km^{-2} yr^{-1}, Fig. 5a) occur in some tropical rivers and regions subjected to intensive agriculture and urbanization, implying that these river systems are important source areas for mitigating riverine N_2O emissions globally. Model forecasts indicate that reduction in riverine DIN loads via improved agricultural N utilization efficiency (i.e., scenario AM, Alcamo *et al.*, 2005) is necessary to decrease global riverine N_2O emission rates by 2050 (Fig. 6). Agricultural N utilization efficiency may be improved by increasing crop yields, enhanced crop growth associated with increased stress tolerance of modern hybrids, matching spatial/temporal plant nutrient demands with precision nutrient application, and enhancing management practices such as conservation tillage,

cover crops and higher plant densities (Cassman *et al.*, 2002). Considering the large future increases of riverine N_2O emission rates projected in South America and Africa as well as subtropical/tropical zones under all scenarios, these two continents and climate zones may be specifically targeted for enhanced mitigation efforts in the future.

Although this study probably tends to overestimate N_2O emission rates for high latitude rivers that are frozen at times of year when N_2O emissions are likely negligible (Baulch *et al.*, 2011), the estimated global riverine N_2O emission rate of 32.2 Gg N_2O–N yr^{-1} in this study is still considerably lower than previous estimates (300–2100 Gg N_2O–N yr^{-1}, Table 3) as well as a recent estimate (194 Gg N_2O–N yr^{-1}) based on the average N_2O fluxes in different latitudinal ranges (Soued *et al.*, 2016). There are two primary reasons for the large difference found in this study. First, global riverine N loads in previous studies were far higher than those used in this study (Table 3). If we use the estimated global mean emission factor value of 0.17% in this study and previous estimates for riverine N loads (Table 3), the global riverine N_2O emission rate would total 63–163 Gg N_2O–N yr^{-1}, which is more comparable to previous estimates. It should be pointed out that three studies using IPCC methods (i.e., the product of a fixed export fraction of 0.3 and estimates of synthetic fertilizer and manure N application) and one study using the NEWS model estimated global total N loads (Table 3) that were 2–5 twofold to fivefold higher than the DIN loads estimated from the NEWS2-DIN-S model in this study. However, using a fixed export fraction in the IPCC method without rigorous calibration and validation ignores potentially large differences in N delivery efficiencies over space and time at the global scale (Nevison, 2000). Therefore, previous compilations may overestimate global total N loads compared to the recent estimates by Kroeze *et al.* (2010) using the NEWS model (a global spatially explicit model with calibration and validation). Previous estimates of global riverine DIN loads from the NEWS model were believed to overestimate DIN loads in arid and tropical regions by not considering their greater N retention efficiencies. In contrast, DIN estimates used in this study were from the NEWS2-DIN-S model that considers seasonal patterns and controls (i.e., runoff and temperature) for DIN delivery; thus, it is considered more reliable and accurate in terms of calibrated model performance (McCrackin *et al.*, 2014).

Second, the EF(a) and EF(b) values used in our study represent the average N_2O emission factor of the N load derived from sewage, leaching and runoff and therefore would be expected to predict inherently lower N_2O emission factors than the EF_{5-r} method that

Table 3 Comparisons of global nitrogen loads, riverine N$_2$O emission factors and emission rates estimated in previous studies and this study

Previous estimations	Nitrogen load estimate methods (N load Tg N yr⁻¹)	Emission factor (%)	Emission rate (Gg N$_2$O-N yr⁻¹)	Remarks
Seitzinger & Kroeze (1998) and Seitzinger et al. (2000)	NEWS model (41.6 for DIN)	2.5	1050 [190, 1870]	Based on four studies with 0.3% and 3% (N$_2$O : N$_2$) for DIN load of <10 and >10 kg N ha⁻¹ yr⁻¹, respectively
Kroeze et al. (2005)	NEWS model (50.3 for DIN)	2.5	1256	Same as Seitzinger & Kroeze (1998)
Mosier et al. (1998)	IPCC method (93 for TN)	0.75	700	Based on six studies made in Europe and North America
De Klein et al. (2006)	IPCC method (93 for TN)	0.25	350	Based on two studies in England and New Zealand for relatively short river systems
Kroeze et al. (2010)	NEWS model (88 for TN 60 for TDN)	0.25 or 2.5	300–2100	IPCC default EF$_{5\text{-}r}$ (0.25%) was used for low case and 2.5% was assumed as the high case based on Seitzinger & Kroeze (1998)
Beaulieu et al. (2011)	IPCC method (90 for TN)	0.75	680	Based on observations conducted for 72 headwater streams in North America with 0.25% observed for denitrification and 0.5% assumed for nitrification
This study	NEWS model (18.8 for DIN)	0.17* [0.08–0.31]	32.2* [12.4–66.9]	Based on meta-analysis of global data with 169 observations covering a wide range of rivers

Total N (TN); dissolved total N (TDN); dissolved inorganic N (DIN).
*Average from four modeling approaches.

represents the average N$_2$O emission factor of the N load from leaching and runoff (i.e., no sewage discharge). In fact, the estimated global mean emission factor of 0.17% in this study is far lower than that used in previous studies (Table 3). Previous studies typically used a constant EF$_{5\text{-}r}$ or emission efficiency factor that was a positive linear function of N load for estimating global or regional riverine N$_2$O emission rates (Table 3). These approaches ignore the pattern of declining EF(a) and EF(b) with increasing DIN levels and channel size (Table S2) and therefore may lead to an overestimation of N$_2$O emission rates for large rivers with high DIN levels. For example, constant N$_2$O : N$_2$ ratios of 0.3% and 3% for rivers with low and high DIN loadings were used in Seitzinger & Kroeze (1998), Seitzinger et al. (2000) and Kroeze et al. (2005). Such assumptions are also subject to a high degree of uncertainty given the two orders of magnitude variability in observed in-stream N$_2$O : N$_2$ ratios (i.e., 0.04–6%, O'Brien et al., 2007; Beaulieu et al., 2011; Yan et al., 2012). Estimates based on global riverine TN or TDN loads also ignore the lower N$_2$O emission factor for organic N than for DIN that is readily available to microbes. The recommended global mean emission factor of 0.75% based on observations from 72 streams with different land-use types in the United States (Beaulieu et al., 2011) might also overestimate because these data were obtained from headwater streams having small channel size and discharge (<1.4 m^3 s^{-1}). Due to the pattern of declining EF(a) and EF(b) with increasing water discharge or channel size and N levels observed in this study (Table S2), directly extrapolating emission factors from observations conducted for headwater streams with lower N levels and smaller channel sizes will greatly overestimate regional or global riverine N$_2$O emission rates as well as emission factors.

Compared to previous global estimates based on limited and localized N$_2$O emission rates (Table 3), this study incorporated diverse information from 169 global rivers located on six continents, three climate zones and covering a large range in water discharge and N levels (Figs 2 and 3). As a result, the observed nonlinear negative relationship between EF(a) or EF(b) and N level, as well as water discharge that was not explored in previous studies due to limited observations, should be more representative for a global scale analysis. Importantly, the four modeling approaches (global and climate stratified with EF(a) and EF(b) stratified) for estimating global riverine N$_2$O emission rates performed well in predicted vs. measured comparisons (Fig. 4), as well as consistency between the four modeling approaches (Table 3). Therefore, this study is believed to offer more accurate global estimates than previous studies and

improves our understanding of factors controlling global riverine N$_2$O emissions.

Suggestions for improving estimates of global riverine N$_2$O emissions

Although this study adopted three emission factor approaches (Table 1, the EF(c) method was not feasible in this analysis due to the unavailability of required data for most rivers, Fig. S5), they undoubtedly incorporate some uncertainties for estimating global riverine N$_2$O emissions. The EF(b) method (i.e., the ratio of riverine N$_2$O to DIN concentrations) might underestimate actual N$_2$O emission factors because it assumes conservative processing of both N$_2$O and DIN in the water column and N$_2$O loss to the atmosphere can occur before the water reaches the sampling sites (Well *et al.*, 2005; Outram & Hiscock, 2012). However, others suggest that EF(b) will overestimate actual N$_2$O emission factors because N$_2$O in the water column is not released to the atmosphere until dissolved N$_2$O supersaturation occurs (Beaulieu *et al.*, 2008). Therefore, rivers with low DIN concentrations and near equilibrium with respect to atmospheric N$_2$O concentrations (especially forest rivers) would be overestimated by the EF (b) approach (Beaulieu *et al.*, 2008; Baulch *et al.*, 2012). However, no significant differences were observed between estimated EF(b) and EF(a) values (Fig. S4), as well as between modeled results based on EF(b) and EF(a) methods (Fig. 4 and Table 2), implying that any underestimation/overestimation potentials might coexist in estimated EF(a)/EF(b) values and/or there was the uncertainty associated with estimated EF(a) values. Although the EF(a) (i.e., the ratio of N$_2$O emission rate to DIN load) is a rigorous method for calculation of global or regional riverine N$_2$O emissions (Well *et al.*, 2005), estimated EF(a) values as well as the models developed in this study might imply some uncertainty due to difficulty in obtaining reliable water surface area and N$_2$O flux data for an entire river network from literature sources. Therefore, more field observations of EF(a) based on rigorous measurements of riverine N$_2$O emission rates and N loads across various continents, climate zones, land-use types and river order (i.e., size) are required for further refining and verifying the developed models. Considering the inherent heterogeneity of natural and anthropogenic attributes, extending measurements of N$_2$O emission rates and emission factors throughout an entire river network is necessary. In addition to spatial variability, temporal variability (e.g., diurnal, storm event and seasonal) in riverine N$_2$O fluxes and emission factors has been widely demonstrated (Laursen & Seitzinger, 2004; Clough *et al.*, 2007; Gonçalves *et al.*, 2010; Yang *et al.*,

2011). Thus, appropriate temporal sampling strategies must be developed to assure that representative N$_2$O emission rates and emission factors have been measured. Furthermore, the mixed use of TN, TDN and DIN loads in previous estimates of global riverine N$_2$O emission rates (Table 3) also confuses the definition and application of emission factors (i.e., they are likely very different for TN, TDN and DIN loads due to their bioavailability). International cooperative studies using standardized methodologies are necessary to refine and verify emission factor methods (EF(a) vs. EF(b) vs. EF(c) and TN vs. TDN vs. DIN). The twofold to threefold variability among estimated global riverine DIN loads (Table 3) highlights the uncertainty in estimates of riverine DIN loads at the global scale. Therefore, it is essential to improve estimates of riverine DIN loads through enhanced monitoring and modeling efforts.

Acknowledgements

References

Aguilera R, Marcé R, Sabater S (2013) Modeling nutrient retention at the watershed scale: does small stream research apply to the whole river network? *Journal of Geophysical Research: Biogeosciences*, **118**, 728–740.

Alcamo J, Vuuren DV, Cramer W *et al.* (2005) Changes in ecosystem services and their drivers across the scenarios. *Ecosystems and Human Well-Being*, **2**, 297–373.

Alexander RB, Smith RA, Schwarz GE (2000) Effect of stream channel size on the delivery of nitrogen to the Gulf of Mexico. *Nature*, **403**, 758–761.

Arango C, Tank JL (2008) Land use influences the spatiotemporal controls on nitrification and denitrification in headwater streams. *Journal of the North American Benthological Society*, **27**, 90–107.

Barnard R, Leadley PW, Hungate BA (2005) Global change, nitrification, and denitrification: a review. *Global Biogeochemical Cycles*, **19**, 1–13.

Barnes J, Owens NJP (1999) Denitrification and nitrous oxide concentrations in the Humber estuary, UK, and adjacent coastal zones. *Marine Pollution Bulletin*, **37**, 247–260.

Baulch HM, Schiff SL, Maranger R, Dillon PJ (2011) Nitrogen enrichment and the emission of nitrous oxide from streams. *Global Biogeochemical Cycles*, **25**, GB4013.

Baulch HM, Dillon PJ, Maranger R, Venkiteswaran JJ, Wilson HF, Schiff SL (2012) Night and day: short-term variation in nitrogen chemistry and nitrous oxide emissions from streams. *Freshwater Biology*, **57**, 509–525.

Beauchamp EG, Trevors JT, Paul JW (1989) Carbon sources for bacterial denitrification. *Advances in Soil Science*, **10**, 113–142.

Beaulieu JJ, Arango CP, Hamilton SK, Tank JL (2008) The production and emission of nitrous oxide from headwater streams in the Midwestern United States. *Global Change Biology*, **14**, 878–894.

Beaulieu J, Shuster WD, Rebholz JA (2010) Nitrous oxide emissions from a large, impounded river: the Ohio River. *Environmental Science & Technology*, **44**, 7527–7533.

Beaulieu JJ, Tank JL, Hamilton SK *et al.* (2011) Nitrous oxide emission from denitrification in stream and river networks. *Proceedings of the National Academy of Sciences*, **108**, 214–219.

Bernot MJ, Dodds WK (2005) Nitrogen retention, removal, and saturation in lotic ecosystems. *Ecosystems*, **8**, 442–453.

Bernot MJ, Tank JL, Royer TV, David MB (2006) Nutrient uptake in streams draining agricultural catchments of the midwestern United States. *Freshwater Biology*, **51**, 499–509.

Boyer EW, Howarth RW, Galloway JN, Dentener FJ, Green PA (2006) Riverine nitrogen export from the continents to the coasts. *Global Biogeochemical Cycles*, **20**, GB1S91

Cassman KG, Dobermann A, Walters DT (2002) Agroecosystems, nitrogen-use efficiency, and nitrogen management. *AMBIO: A Journal of the Human Environment*, **31**, 132–140.

Cébron A, Garnier J, Billen G (2005) Nitrous oxide production and nitrification kinetics by natural bacterial communities of the lower Seine river (France). *Aquatic Microbial Ecology*, **41**, 25–38.

Chen D, Lu J, Shen Y, Gong D, Deng O (2011) Spatio-temporal variations of nitrogen in an agricultural watershed in eastern China: catchment export, stream attenuation and discharge. *Environmental Pollution*, **159**, 2989–2995.

Christensen PB, Nielsen LP, Sørensen J, Revsbech NP (1990) Denitrification in nitrate-rich streams: diurnal and seasonal variation related to benthic oxygen metabolism. *Limnology and Oceanography*, **35**, 640–651.

Clough TJ, Bertram JE, Sherlock RR, Leonard RL, Nowicki BL (2006) Comparison of measured and EF5-r-derived N$_2$O fluxes from a spring-fed river. *Global Change Biology*, **12**, 352–363.

Clough TJ, Buckthought LE, Kelliher FM, Sherlock RR (2007) Diurnal fluctuations of dissolved nitrous oxide (N$_2$O) concentrations and estimates of N$_2$O emissions from a spring-fed river: implications for IPCC methodology. *Global Change Biology*, **13**, 1016–1027.

Clough TJ, Buckthought LE, Casciotti KL, Kelliher FM, Jones PK (2011) Nitrous oxide dynamics in a braided river system, New Zealand. *Journal of Environmental Quality*, **40**, 1532–1541.

Cole JJ, Caraco NF (2001) Emissions of nitrous oxide (N$_2$O) from a tidal, freshwater river, the Hudson River, New York. *Environmental Science & Technology*, **35**, 991–996.

De Klein C, Novoa RSA, Ogle S et al. (2006) Chapter 11: N$_2$O emissions from managed soils, and CO$_2$ emissions from lime and urea application. In: *Agriculture, Forestry and Other Land Use, 2006 IPCC Guidelines for National Greenhouse Gas Inventories*, Vol **4** (eds Eggleston S, Buendia L, Miwa K, Ngara T, Tanabe K), pp. 11.1–11.54. Institute for Global Environmental Strategies, Japan.

Dong LF, Nedwell DB, Colbeck I, Finch J (2005) Nitrous oxide emission from some English and Welsh rivers and estuaries. *Water, Air & Soil Pollution: Focus*, **4**, 127–134.

Doorn MRJ, Towprayoon S, Vieira SMM et al. (2006) Chapter 6: Wastewater treatment and discharge. In: *Waste, 2006 IPCC Guidelines for National Greenhouse Gas Inventories*, Vol **5** (eds Eggleston S, Buendia L, Miwa K, Ngara T, Tanabe K), pp. 6.1–6.21. Institute for Global Environmental Strategies, Hayama, Japan.

Dumont E, Harrison JA, Kroeze C, Bakker EJ, Seitzinger SP (2005) Global distribution and sources of dissolved inorganic nitrogen export to the coastal zone: results from a spatially explicit, global model. *Global Biogeochemical Cycles*, **19**, GB4S02

Galloway JN, Dentener FJ, Capone DG et al. (2004) Nitrogen cycles: past, present, and future. *Biogeochemistry*, **70**, 153–226.

Garnier J, Billen G, Vilain G, Martinez A, Silvestre M, Mounier E, Toche F (2009) Nitrous oxide (N$_2$O) in the Seine river and basin: observations and budgets. *Agriculture, Ecosystems & Environment*, **133**, 223–233.

Gonçalves C, Brogueira MJ, Camões MF (2010) Seasonal and tidal influence on the variability of nitrous oxide in the Tagus estuary, Portugal. *Scientia Marina*, **74**, 57–66.

Green PA, Vörösmarty CJ, Meybeck M, Galloway JN, Peterson BJ, Boyer EW (2004) Pre-industrial and contemporary fluxes of nitrogen through rivers: a global assessment based on typology. *Biogeochemistry*, **68**, 71–105.

Harley JF, Carvalho L, Dudley B, Heal KV, Rees RM, Skiba U (2015) Spatial and seasonal fluxes of the greenhouse gases N$_2$O, CO$_2$ and CH$_4$ in a UK macrotidal estuary. *Estuarine, Coastal and Shelf Science*, **153**, 62–73.

Hartmann DL, Klein TAMG., Rusicucci M et al. (2013) *Observations: Atmosphere and surface. Climate Change 2013: The Physical Science Basis, Intergovernmental Panel on Climate Change*, pp. 159–254. Cambridge Univ. Press, New York.

Hedin LO, von Fischer JC, Ostrom NE, Kennedy BP, Brown MG, Robertson GP (1998) Thermodynamic constraints on nitrogen transformations and other biogeochemical processes at soil–stream interfaces. *Ecology*, **79**, 684–703.

Hemond HF, Duran AP (1989) Fluxes of N$_2$O at the sediment-water and water-atmosphere boundaries of a nitrogen-rich river. *Water Resources Research*, **25**, 839–846.

Her JJ, Huang JS (1995) Influences of carbon source and C/N ratio on nitrate/nitrite denitrification and carbon breakthrough. *Bioresource Technology*, **54**, 45–51.

Hinshaw SE, Dahlgren RA (2013) Dissolved nitrous oxide concentrations and fluxes from the eutrophic San Joaquin River, California. *Environmental Science & Technology*, **47**, 1313–1322.

Holmes RM, Jones JB Jr, Fisher SG, Grimm NB (1996) Denitrification in a nitrogen-limited stream ecosystem. *Biogeochemistry*, **33**, 125–146.

Ivens WP, Tysmans DJ, Kroeze C, Löhr AJ, Wijnen JV (2011) Modeling global N$_2$O emissions from aquatic systems. *Current Opinion in Environmental Sustainability*, **3**, 350–358.

Kroeze C, Dumont E, Seitzinger SP (2005) New estimates of global emissions of N$_2$O from rivers and estuaries. *Environmental Sciences*, **2**, 159–165.

Kroeze C, Dumont E, Seitzinger SP (2010) Future trends in emissions of N$_2$O from rivers and estuaries. *Journal of Integrative Environmental Sciences*, **7**, 71–78.

Laursen AE, Seitzinger SP (2002) Measurement of denitrification in rivers: an integrated, whole reach approach. *Hydrobiologia*, **485**, 67–81.

Laursen AE, Seitzinger SP (2004) Diurnal patterns of denitrification, oxygen consumption and nitrous oxide production in rivers measured at the whole-reach scale. *Freshwater Biology*, **49**, 1448–1458.

Liu X, Zhang Y, Han W et al. (2013) Enhanced nitrogen deposition over China. *Nature*, **494**, 459–462.

Matson P, Lohse KA, Hall SJ (2002) The globalization of nitrogen deposition: consequences for terrestrial ecosystems. *AMBIO: A Journal of the Human Environment*, **31**, 113–119.

McCrackin ML, Harrison JA, Compton JE (2014) Factors influencing export of dissolved inorganic nitrogen by major rivers: a new, seasonal, spatially explicit, global model. *Global Biogeochemical Cycles*, **28**, 269–285.

McMahon P, Dennehy K (1999) N$_2$O emissions from a nitrogen-enriched river. *Environmental Science & Technology*, **33**, 21–25.

Miller MN, Zebarth BJ, Dandie CE, Burton DL, Goyer C, Trevors JT (2008) Crop residue influence on denitrification, N$_2$O emissions and denitrifier community abundance in soil. *Soil Biology and Biochemistry*, **40**, 2553–2562.

Mosier A, Kroeze C, Nevison C, Oenema O, Seitzinger S, Cleemput OV (1998) Closing the global N$_2$O budget: nitrous oxide emissions through the agricultural nitrogen cycle. *Nutrient Cycling in Agroecosystems*, **52**, 225–248.

Mulholland PJ, Helton AM, Poole GC et al. (2008) Stream denitrification across biomes and its response to anthropogenic nitrate loading. *Nature*, **452**, 202–205.

Mulholland PJ, Hall RO, Sobota DJ et al. (2009) Nitrate removal in stream ecosystems measured by 15N addition experiments: denitrification. *Limnology and Oceanography*, **54**, 666–680.

Nevison C (2000) Review of the IPCC methodology for estimating nitrous oxide emissions associated with agricultural leaching and runoff. *Chemosphere-Global Change Science*, **2**, 493–500.

O'Brien JM, Dodds WK, Wilson KC, Murdock JN, Eichmiller J (2007) The saturation of N cycling in Central Plains streams: 15N experiments across a broad gradient of nitrate concentrations. *Biogeochemistry*, **84**, 31–49.

Outram FN, Hiscock KM (2012) Indirect nitrous oxide emissions from surface water bodies in a lowland arable catchment: a significant contribution to agricultural greenhouse gas budgets? *Environmental Science & Technology*, **46**, 8156–8163.

Payne WJ (1981) *Denitrification*. John Wiley & Sons Inc., New York.

Peterson BJ, Wollheim WM, Mulholland PJ et al. (2001) Control of nitrogen export from watersheds by headwater streams. *Science*, **292**, 86–90.

Raymond PA, Cole JJ (2001) Gas exchange in rivers and estuaries: choosing a gas transfer velocity. *Estuaries and Coasts*, **24**, 312–317.

Raymond PA, Zappa CJ, Butman D et al. (2012) Scaling the gas transfer velocity and hydraulic geometry in streams and small rivers. *Limnology and Oceanography: Fluids and Environments*, **2**, 41–53.

Reay DS, Smith KA, Edwards AC (2003) Nitrous oxide emission from agricultural drainage waters. *Global Change Biology*, **9**, 195–203.

Rosamond MS, Thuss SJ, Schiff SL (2012) Dependence of riverine nitrous oxide emissions on dissolved oxygen levels. *Nature Geoscience*, **5**, 715–718.

Seitzinger SP, Kroeze C (1998) Global distribution of nitrous oxide production and N inputs in freshwater and coastal marine ecosystems. *Global Biogeochemical Cycles*, **12**, 93–113.

Seitzinger SP, Kroeze C, Styles RV (2000) Global distribution of N$_2$O emissions from aquatic systems: natural emissions and anthropogenic effects. *Chemosphere-Global Change Science*, **2**, 267–279.

Sobczak WV, Findlay S, Dye S (2003) Relationships between DOC bioavailability and nitrate removal in an upland stream: an experimental approach. *Biogeochemistry*, **62**, 309–327.

Soued C, del Giorgio PA, Maranger R (2016) Nitrous oxide sinks and emissions in boreal aquatic networks in Québec. *Nature Geoscience*, **9**, 116–120.

Stow CA, Walker JT, Cardoch L, Spence P, Geron C (2005) N$_2$O emissions from streams in the Neuse River watershed, North Carolina. *Environmental Science & Technology*, **39**, 6999–7004.

Syakila A, Kroeze C (2011) The global nitrous oxide budget revisited. *Greenhouse Gas Measurement and Management*, **1**, 17–26.

Toyoda S, Iwai H, Koba K, Yoshida N (2009) Isotopomeric analysis of N$_2$O dissolved in a river in the Tokyo metropolitan area. *Rapid Communications in Mass Spectrometry*, **23**, 809–821.

Turner PA, Griffis TJ, Lee X, Baker JM, Venterea RT, Wood JD (2015) Indirect nitrous oxide emissions from streams within the US Corn Belt scale with stream order. *Proceedings of the National Academy of Sciences*, **112**, 9839–9843.

Van Den Heuvel RN, Bakker SE, Jetten MSM, Hefting MM (2011) Decreased N$_2$O reduction by low soil pH causes high N$_2$O emissions in a riparian ecosystem. *Geobiology*, **9**, 294–300.

Venkiteswaran JJ, Rosamond MS, Schiff SL (2014) Nonlinear response of riverine N$_2$O fluxes to oxygen and temperature. *Environmental Science & Technology*, **48**, 1566–1573.

Wang J, Chen N, Yan W, Wang B, Yang L (2015) Effect of dissolved oxygen and nitrogen on emission of N$_2$O from rivers in China. *Atmospheric Environment*, **103**, 347–356.

Webster JR, Mulholland PJ, Tank JL *et al.* (2003) Factors affecting ammonium uptake in streams – an inter-biome perspective. *Freshwater Biology*, **48**, 1329–1352.

Weiss RF, Price BA (1980) Nitrous oxide solubility in water and seawater. *Marine Chemistry*, **8**, 347–359.

Well R, Weymann D, Flessa H (2005) Recent research progress on the significance of aquatic systems for indirect agricultural N$_2$O emissions. *Environmental Sciences*, **2**, 143–151.

Xia Y, Li Y, Li X, Guo M, She D, Yan X (2013) Diurnal pattern in nitrous oxide emissions from a sewage-enriched river. *Chemosphere*, **92**, 421–428.

Yan W, Yang L, Wang F, Wang J, Ma P (2012) Riverine N$_2$O concentrations, exports to estuary and emissions to atmosphere from the Changjiang River in response to increasing nitrogen loads. *Global Biogeochemical Cycles*, **26**, GB4006.

Yang L, Yan W, Ma P, Wang J (2011) Seasonal and diurnal variations in N$_2$O concentrations and fluxes from three eutrophic rivers in Southeast China. *Journal of Geographical Sciences*, **21**, 820–832.

Yu Z, Deng H, Wang D *et al.* (2013) Nitrous oxide emissions in the Shanghai river network: implications for the effects of urban sewage and IPCC methodology. *Global Change Biology*, **19**, 2999–3010.

Zarnetske JP, Haggerty R, Wondzell SM, Bokil VA, González-Pinzón R (2012) Coupled transport and reaction kinetics control the nitrate source-sink function of hyporheic zones. *Water Resources Research*, **48**, W11508.

Supporting Information

Additional Supporting Information may be found in the online version of this article:

Data S1. Data source and characteristics.

Figure S1. Selected study sites (n = 169) used in this study.

Figure S2. Histogram of (a) EF(a), (b) EF(b) and (c) N$_2$O emission flux.

Figure S3. Box plots of N$_2$O emission fluxes from lake/reservoir, river, wetland, and soil. Lower letters above bars denote significant differences ($P < 0.01$).

Table S1. The characteristics of compiled data for this meta-analysis.

Data S2. Calculation and evaluation of EF(c).

Figure S4. (a) Box plot of EF(a), EF(b) and EF(c); (b) comparison among N$_2$O flux estimated from EF(c) and EF(b) compared to the N$_2$O flux measured in the field. Lower case letters above bars denote significant differences ($P < 0.05$) according to one-way ANOVA after logarithmic transformation.

Figure S5. Histogram of sensitivity analysis result for $C_{\text{equilibrium}}$.

Data S3. Regression analyses for river N$_2$O emission.

Table S2. Single factor regression analyses for river N$_2$O emission flux (μg N$_2$O–N m^{-2} h^{-1}), emission factors (i.e., EF(a) and EF(b)) and various influencing factors for global data.

Table S3. Single factor regression analyses for river N$_2$O emission flux (μg N$_2$O–N m^{-2} h^{-1}), emission factor (EF(a) and EF(b)) and various influencing factors by land-use types.

Table S4. Single factor regression analyses for river N$_2$O emission flux (μg N$_2$O–N m^{-2} h^{-1}), emission factor (EF(a) and EF(b)), and various influencing factors by climate zones.

Table S5. Multiple regression models for predicting river N$_2$O emission factor (EF(a)) and emission rate (ER, kg N$_2$O–N yr^{-1}) using 82 combinations of nitrate (C_{N}, mg N L^{-1}), ammonium (C_{A}, mg N L^{-1}), DIN (C_{DIN}, mg N L^{-1}) and DOC concentration (C_{DOC}, mg C L^{-1}), DOC : DIN ratio (R), discharge (Q, m^3 s^{-1}), nitrate (Y_{N}, kg N yr^{-1} km^{-2}), ammonium (Y_{A}, kg N yr^{-1} km^{-2}), and DIN yield (Y_{DIN}, kg N yr^{-1} km^{-2}), nitrate (L_{N}, kg N yr^{-1}), ammonium (L_{A}, kg N yr^{-1}), and DIN load (L_{DIN}, kg N yr^{-1}) for global data.

Table S6. Multiple regression models for predicting river N$_2$O emission factor (EF(a)) and emission rate (ER$_{\text{st}}$, kg N$_2$O–N yr^{-1}) using 82 combinations of nitrate (C_{N}, mg N L^{-1}), ammonium (C_{A}, mg N L^{-1}), DIN (C_{DIN}, mg N L^{-1}) and DOC concentration (C_{DOC}, mg C L^{-1}), DOC : DIN ratio (R), discharge (Q, m^3 s^{-1}), nitrate (Y_{N}, kg N yr^{-1} km^{-2}), ammonium (Y_{A}, kg N yr^{-1} km^{-2}), and DIN yield (Y_{DIN}, kg N yr^{-1} km^{-2}), nitrate (L_{N}, kg N yr^{-1}), ammonium (L_{A}, kg N yr^{-1}), and DIN load (L_{DIN}, kg N yr^{-1}) for sub-tropical/tropical zones data.

Table S7. Multiple regression models for predicting river N$_2$O emission factor (EF(a)) and emission rate (ER$_{\text{t}}$, kg N$_2$O–N yr^{-1}) using 82 combinations of nitrate (C_{N}, mg N L^{-1}), ammonium (C_{A}, mg N L^{-1}), DIN (C_{DIN}, mg N L^{-1}) and DOC concentration (C_{DOC}, mg C L^{-1}), DOC : DIN ratio (R), discharge (Q, m^3 s^{-1}), nitrate (Y_{N}, kg N yr^{-1} km^{-2}), ammonium (Y_{A}, kg N yr^{-1} km^{-2}), and DIN yield (Y_{DIN}, kg N yr^{-1} km^{-2}), nitrate (L_{N}, kg N yr^{-1}), ammonium (L_{A}, kg N yr^{-1}), and DIN load (L_{DIN}, kg N yr^{-1}) for temperate zone data.

Table S8. Multiple regression models for predicting river N$_2$O emission factor (EF(b)) and emission rate (ER, kg N$_2$O–N yr^{-1}) using 82 combinations of nitrate (C_{N}, mg N L^{-1}), ammonium (C_{A}, mg N L^{-1}), DIN (C_{DIN}, mg N L^{-1}) and DOC concentration (C_{DOC}, mg C L^{-1}), DOC : DIN ratio (R), discharge (Q, m^3 s^{-1}), nitrate (Y_{N}, kg N yr^{-1} km^{-2}), ammonium (Y_{A}, kg N yr^{-1} km^{-2}), and DIN yield (Y_{DIN}, kg N yr^{-1} km^{-2}), nitrate (L_{N}, kg N yr^{-1}), ammonium (L_{A}, kg N yr^{-1}), and DIN load (L_{DIN}, kg N yr^{-1}) for global data.

Table S9. Multiple regression models for predicting river N$_2$O emission factor (EF(b)) and emission rate (ER$_{st}$, kg N$_2$O–N yr^{-1}) using 82 combinations of nitrate (C_N, mg N L^{-1}), ammonium (C_A, mg N L^{-1}), DIN (C_{DIN}, mg N L^{-1}) and DOC concentration (C_{DOC}, mg C L^{-1}), DOC : DIN ratio (R), discharge (Q, m^3 s^{-1}), nitrate (Y_N, kg N yr^{-1} km^{-2}), ammonium (Y_A, kg N yr^{-1} km^{-2}), and DIN yield (Y_{DIN}, kg N yr^{-1} km^{-2}), nitrate (L_N, kg N yr^{-1}), ammonium (L_A, kg N yr^{-1}), and DIN load (L_{DIN}, kg N yr^{-1}) for sub-tropical/tropical zones data.

Table S10. Multiple regression models for predicting river N$_2$O emission factor (EF(b)) and emission rate (ER$_t$, kg N$_2$O–N yr^{-1}) using 82 combinations of nitrate (C_N, mg N L^{-1}), ammonium (C_A, mg N L^{-1}), DIN (C_{DIN}, mg N L^{-1}) and DOC concentration (C_{DOC}, mg C L^{-1}), DOC : DIN ratio (R), discharge (Q, m^3 s^{-1}), nitrate (Y_N, kg N yr^{-1} km^{-2}), ammonium (Y_A, kg N yr^{-1} km^{-2}), and DIN yield (Y_{DIN}, kg N yr^{-1} km^{-2}), nitrate (L_N, kg N yr^{-1}), ammonium (L_A, kg N yr^{-1}), and DIN load (L_{DIN}, kg N yr^{-1}) for temperate zone data.

Data S4. Estimation of global riverine DIN load.

Data S5. Estimation of global river N$_2$O emission and uncertainty analysis.

Data S6. Prediction of future riverine DIN loads under Millennium Ecosystem Assessment scenarios.

Table S11. Future (2000–2050) trends in global riverine DIN loads by continent and climate zone.